Ice ablation by pyroclast impact during subglacial fragmentation-dominated eruptions

Duncan Woodcock, Jennie Gilbert, Stephen Lane, and Lionel Wilson
Lancaster Environment Centre, Lancaster University, Lancaster, LA1 4YQ, UK
Corresponding author: duncan.woodcock@hotmail.co.uk

Abstract

Understanding magma-ice interaction processes is critical for mitigation of the hazards generated by subglacial explosive volcanism, including large flowrate meltwater floods and fine-grained volcanic ash. We propose and evaluate a subglacial eruption mechanism with potential for rapid ablation of the overlying ice that involves the impact of pyroclasts on the ice surfaces of depressurised, vapour dominated ice cavities that surround subglacial vents. Such impacts are likely to cause considerable fracturing and mechanical fragmentation of the ice and thus increase the heat transfer area available for ice-melt. This mechanism has not, to our knowledge, been explored previously in the literature, but we find that published experimental work on impact cratering of icy solar system bodies can be used to predict fragmentation damage by pyroclast impact. Our principal conclusions are as follows. (1) Ice ablation rates of order 100 m h^{-1} are predicted, for typical pyroclast velocities, provided that the mechanism is sustained. (2) The thermal energy of the eruption, together with the size of the ice fragments produced, is sufficient to prevent accumulation of fractured ice within the cavity. (3) Upward ablation of the ice cavity roof results in a progressive decrease in pyroclast impact velocity that is partly compensated by downward movement of the roof by ductile ice flow. (4) This ice ablation mechanism is likely common during subglacial eruptions on the relatively steep slopes of ice-covered stratovolcanoes, where steepness of slope and ice

thickness are favourable for rapid drainage of meltwater by gravity and consequent depressurisation of the cavity.

Keywords: volcano-ice interaction, glaciovolcanism, ice fragmentation, ice-melt, ice ablation, magma-ice heat transfer

1. Introduction

Subglacial eruptions generate hazards that result from the interaction of magma with ice. Fragmentation of magma by explosion (producing pyroclasts) or granulation (producing hyaloclastite) can promote efficient magma-ice heat transfer [*Gudmundsson et al.*, 2004]. The resulting rapid ice-melt can generate large flowrates of meltwater (jökulhlaups) which, together with mobilisation of sediments by the floodwaters, are the most common volcanic hazard in Iceland. These jökulhlaups have caused extensive damage to bridges and other infrastructure as well as repeated evacuations from affected areas [*Gudmundsson et al.*, 2008].

Subglacial eruptions may remove (i.e., ablate) the overlying ice by a combination of melting and fracturing to breach the ice surface and become subaerial [*Gudmundsson*, 2003]. The resulting volcanic plumes present a variety of proximal to distal hazards. In particular, the interaction of magma with meltwater may produce fine-grained ash that is carried upwards by the plume and disperses widely in the atmosphere. Under conditions of adverse wind direction airborne volcanic ash may lead to restrictions on air traffic and subsequent disruption to global air travel and supply chains, such as those experienced during the Eyjafjallajökull 2010 eruption in Iceland [*Dellino et al.*, 2012; *Harris et al.*, 2012].

Volcano-ice interaction around an erupting vent produces a fluid-filled cavity at the base of the ice sheet. Within this ice cavity, the processes involved in subglacial fragmentation-dominated eruptions may include vigorous fluid convection with heat transfer to the ice from liquid water or steam (i.e., water in the vapour phase) and, in some cases, the impact of pyroclasts on the icy walls and roof of the subglacial cavity. The key parameter that helps to constrain any model of these subglacial processes is the "ice ablation rate". We use the term "ice ablation" to mean the progressive removal of ice by magma-ice interaction, including (1) ice-melt by magma-ice heat transfer, and (2) mechanical fragmentation of ice due to ice fracturing during direct pyroclast impact. Figure 1 shows the definition of ice ablation rate, together with the observations needed for its determination for a subglacial eruption.

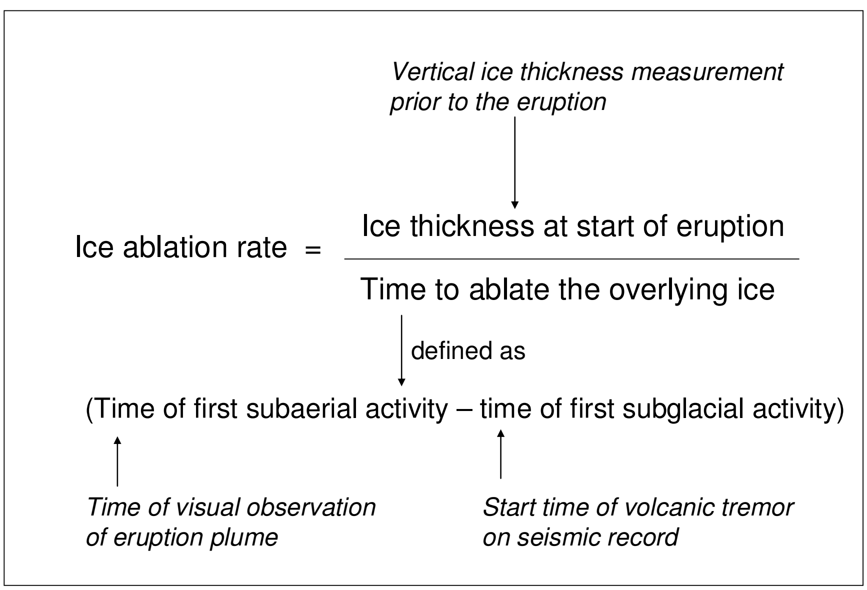

Figure 1. The variables involved in estimating ice ablation rate for a subglacial volcanic eruption. The observations needed for its determination are italicised.

Despite the plethora of ice-covered volcanoes on Earth, there are few published examples of explosive subglacial eruptions where observations enable ice ablation rates to be inferred: these include three Icelandic eruptions [*Gudmundsson et al*., 2004; *Magnússon et al*., 2012; *Larsen et al.,* 2021], together with an example from Antarctica [*Smellie*, 2002]. All of these examples are of mafic or intermediate magmas erupted into temperate ice-sheets or glaciers, where the ice is at its pressure melting point. These eruptions provide the crucial empirical data with which any analytical model of ice ablation rate can be compared. Table 1 summarises the measurements, observations and inferences associated with the estimations of pre-eruption ice thicknesses and the durations of these subglacial eruptions, together with the resulting ice ablation rates.

Table 1. Summary of measurements, observations and inferences that allow estimation of ice ablation rates for selected subglacial eruptions that breached the overlying ice.

Subglacial eruption	Pre-eruption ice thickness	Start time of subglacial eruption	Time of ice surface breach	Duration of subglacial phase of eruption	Approximate ice ablation rate ($m\ h^{-1}$) (range in brackets)
Eyjafjallajökull 2010	Ice thicknesses of 170-200 m were recorded above the 2010 eruption site [*Magnússon et al., 2012*]. No evidence for any pre-eruption melting.	Inferred from start of strong continuous tremor at 0130 h on 14th April [*Magnússon et al.*, 2012].	Eruption plume observed by aircraft at around 0600 h on 14th April [*Magnússon et al.*, 2012].	4 hours	50 (40-50)
Gjálp 1996	550-600 m measured in 1986 [*Gudmundsson et al.*, 2004].	Inferred from start of strong continuous tremor at 2200 h on 30th September [*Gudmundsson et al.*, 2004].	Steam emission observed from ice cauldron at 0447 h on 2nd October, with subaerial phreatomagmatic activity confirmed at 0518 h [*Gudmundsson et al.*, 2004].	31 hours	18 (18-19)
Deception Island 1969	Glacier thickness measurements varied from 100 m to approximately 50 m at snout. Thickness at eruption site estimated at 70-100 m [*Smellie*, 2002].	Inferred from start of continuous tremor at 0750 h or from sudden end to a sequence of multiple small earthquakes at 0915 h on 21st February [*Smellie*, 2002].	Initial observation of eruption column at 0950 h on 21st February [*Smellie*, 2002].	35 minutes-2 hours	100 (50-170)
Katla 1918	270-300 m measured by radio echo-sound at the location of eruption site [*Björnsson et al.,* 2000]. May have been somewhat thicker in 1918, perhaps 350 m [*Gudmundsson et al., 2021*].	Inferred from contemporary observations of seismic activity at 1130 h and first indications of flow of meltwater.at 1300-1330 on 12th October [*Larsen et al.,* 2021].	Eruption plume observed at 1500 h 12th October [*Larsen et al.,* 2021].	2-3.5 hours	130 (85-175)

Theoretical models for magma-water-ice heat transfer during subglacial fragmentation-dominated eruptions were developed by *Woodcock* [2016]. This work demonstrated that, for eruptions where magma becomes fragmented, heat transfer from magma to liquid water is rapid on the timescale of an eruption, at least for small pyroclasts, and thus is unlikely to limit overall magma-ice heat transfer rates [*Woodcock et al.*, 2012]. In addition, ice ablation rates that approach those inferred for the Gjálp 1996 eruption (Iceland) were predicted by a water-ice heat transfer model that involved two-phase convection in liquid-dominated cavities at glaciostatic pressures [*Woodcock et al.*, 2014]. The principal limitation on ice ablation rate in this model was that the area available for water-ice heat transfer was restricted to that of the roof and walls of the ice cavity. In this paper, we propose and evaluate a mechanism where this restriction does not exist.

For ice that is 150-200 m or more thick, water pressure is near glaciostatic most of the time, particularly during the start of subglacial eruptions [*Björnsson*, 1975; *Nye*, 1976; *Gudmundsson et al.*, 2004]. Observations of subglacial eruptions under thick ice in Iceland are consistent with models of heat transfer within a liquid water-dominated cavity under glaciostatic pressure [*Gudmundsson et al.*, 2004, *Magnússon et al.,* 2012]. In contrast, for the thinner ice that may occur on the relatively steep slopes of ice-covered stratovolcanoes, steepness of slope and ice thickness are favourable for rapid drainage of meltwater by gravity, as observed during minor flank eruptions during the 2010 Icelandic eruption at Eyjafjallajökull [*Magnússon et al*. 2012]. Once the vent in such a system is exposed to pressures approaching atmospheric, the eruption effectively becomes subaerial. If water gains access to the depressurised vent, one should expect phreatomagmatic activity in which pyroclasts impact on the roof of the ice cavity [*Wilson and Head*, 2002]. Such impacts are likely to cause considerable mechanical fracturing and fragmentation of the overlying ice and thus increase the heat transfer area available for ice-melt. This scenario, involving ice fragmentation by pyroclast impact, has potential for rapid ablation of the overlying ice and for high rates of ice-melt. It has not, to our knowledge, been explored previously in the literature.

In this paper we explore the fragmentation of the ice roof and walls by the impact of predominantly solid pyroclasts produced during an explosive subglacial eruption within a depressurised subglacial cavity. We begin by reviewing the literature on impact damage to ice surfaces by the high velocity impact of projectiles. We then discuss the relevance of these studies to the impact of large pyroclasts (8 - 64 mm), with velocities of approximately 100 m s^{-1} [*Parfitt and Wilson*, 2008], on the interior of a subglacial ice cavity and estimate the rates of ice removal by impact. In order for such a mechanism to be sustained, the resulting ice fragments need to be removed from the cavity to prevent accumulation; thus, we determine whether meltwater can be generated at a sufficient rate to produce a mixture of pyroclasts, ice and liquid water with sufficient mobility to flow out of the cavity.

2. Ice fragmentation by the impact of large pyroclasts

2.1 Experimental work on impact damage to ice surfaces

There is a considerable body of literature concerned with experimental cratering on ice surfaces by the impact of high velocity projectiles. This work was motivated by the desire to understand the formation of impact craters on ice-dominated bodies in the outer part of the Solar System. Much of the recent experimental work [e.g., *Shrine et al.*, 2002; *Burchell and Johnson,* 2005] was concerned with hypervelocity (1-10 km

s^{-1}) impacts. Earlier studies [*Lange and Ahrens*, 1987; *Kato et al.*, 1995; *Iijima et al.*, 1995] reported the results of medium velocity (0.1-0.6 km s^{-1}) impacts of bullet-sized cylinders on polycrystalline water ice at 255-258 K. These publications include data on projectile mass, density, and velocity, together with the resulting crater dimensions. These data may be used to assess the extent of ice fragmentation by the impact of large pyroclasts if they can be appropriately scaled.

2.1.1 Scaling of experimental results

Dimensional analysis was applied to the scaling of crater sizes by *Holsapple and Schmidt* [1982]. For the strength-dominated regime applicable to small craters produced under Earth gravity conditions [*Holsapple,* 1993], the crater volume V is considered to depend on the radius a, velocity u and density δ of the projectile as well as the material strength Y and density ρ of the target material:

$$V = \mathrm{f}(a, u, \delta, Y, \rho) \qquad (1)$$

The material strength Y is conventionally represented by the compressive strength. *Holsapple* [1993] points out that this is not as restrictive as it seems because all other material strength properties can be expressed in terms of Y if properties are independent of strain rate. In general, ice strength properties are strain rate-dependent [*Paterson*, 2002]; however, under the high strain rates during impact, ice behaves as a brittle material and its behaviour can be considered to be strain rate-independent. Equation (1) has six variables that are expressed in three independent dimensions (mass, length, and time). The Buckingham π theorem [*Middleton and Wilcock*, 1994] indicates that the system behaviour may be described by three dimensionless groups:

$$\frac{\rho\, V}{m} = \mathrm{f}\left(\frac{Y}{\delta\, u^2}, \frac{\rho}{\delta}\right) \qquad (2)$$

where m is the projectile mass (equal to $4 \pi a^3 \delta / 3$ for a spherical projectile). The group $(\rho V) / m$ is the ratio of the mass of cratered material to the mass of the projectile and is known as the cratering efficiency; the group $Y / (\delta u^2)$ is the ratio of target strength to inertial force per unit area of the projectile and the group ρ / δ is the ratio of target density to projectile density.

The functional dependence of the dimensionless groups in equation (2) must be determined by experiment. Figure 2 shows data from *Kato et al.* [1995] and *Iijima et al.* [1995] for the impact of aluminium and basalt projectiles on ice at 255 K. The projectiles used were cylindrical, 15 mm in diameter and 10 mm long, with a mass of around 5 g. The data in Figure 2 may be fitted by the regression line:

$$\frac{\rho V}{m} = 1.15 \left(\frac{\delta u^2}{Y}\right) \qquad (3)$$

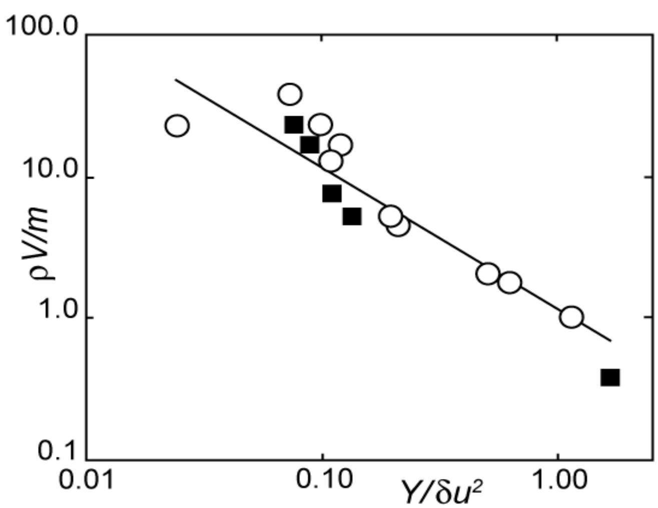

Figure 2. Dimensionless plot of experimental data (from *Kato et al.*, [1995] and *Iijima et al*. [1995]) for the impact of projectiles, with a density ratio (ρ / δ) of 0.31-0.32, on ice at 255 K. Open circles indicate data for aluminium alloy projectiles; filled squares for basalt projectiles. The projectile velocities are in the range 59-290 m s^{-1}. The straight line is the regression line (equation 3).

2.1.2 Ice fragment size distribution

The experiments described in *Kato et al.* [1995] involved firing projectiles vertically downwards onto an upward-facing planar ice surface "target". These experiments were carried out in a cold room at -18 °C to allow recovery of the ice fragments produced during a cratering experiment for the determination of the ice fragment size distribution by dry sieving. For the impact experiments using basaltic projectiles, 80% by mass of the ice fragments were less than 3 mm in size, while 60 % were less than 1 mm. In Section 4 we use this result to estimate the rate at which ice fragments produced by pyroclast impact may melt within the subglacial eruption cavity.

2.2 Relevance to pyroclast impact in subglacial cavities

Table 2 compares the conditions of the experiments reported by *Kato et al.*, [1995] and *Iijima et al.* [1995] with the "requirements" for an analysis of pyroclast impact in subglacial cavities. Differences in projectile size and velocity may be accounted for by equation (3). Data in *Kato et al.* [1995] and *Iijima et al.* [1995] were obtained for ice at 255 K; unfortunately, there are no data available between 255 K and the pressure melting point of ice at 0.1 - 0.2 MPa (approximately 273 K). The compressive strength of ice decreases by a factor of three between 255 K and 273 K [*Croft et al.*,1979; *Petrovic,* 2003]. *Kato et al.* [1995] and *Iijima et al.* [1995] studied ice impact on an upward-facing target. For strength-controlled cratering, orientation should have a minor effect. Craters formed on a downward-facing surface should be no smaller than those scaled from experiments and may be larger as gravity will tend to remove impact fragments rather than allow accumulation in the impact zone.

Table 2. Comparison of experimental conditions reported with the "requirements" for an analysis of pyroclast impact in subglacial cavities.

Variable	Experimental work reported[a]	"Requirements" for subglacial cavity
Regime	Strength-dominated	Strength-dominated
Projectile velocity (m s^{-1})	59 - 290	approximately 100
Projectile size (mm)	7-15	8 - 64
Ice temperature (K)	255	Pressure melting point (approximately 273)
Orientation of ice surface	Upward-facing	Downward-facing
Number of impacts and quality of ice surface	Single impact on pristine planar ice surface	Multiple impacts on damaged ice surface
Nature of projectile	Solid, cold	Variably solidified, but behaves as solid under timescale of impact

[a] *Kato et al.* [1995] and *Iijima et al*. [1995].

So far, we have found no data for multiple impacts at the same site. This is not surprising, since much of the motivation for the work is the study of impacts on icy bodies in the outer Solar System. These bodies lack atmospheres, and it is the stress caused by deceleration through a planetary atmosphere that causes a meteoroid to break up into fragments impacting the same location in quick succession [*Limonta et al*., 2021]. Nevertheless, comparison of the sizes of craters produced by impacts with the same energy into targets of the same material in either solid or fractured form [*Susorney et al*., 2017] imply that impacts into already-fractured ice may produce larger ice craters than expected from equation (3).

3. Application of experimental work to ice fragmentation by pyroclast impact during explosive subglacial eruptions

3.1 Subglacial eruption scenario

We envisage a subglacial explosive fissure eruption within a vapour-dominated ice cavity, with a pressure of 0.1-0.2 MPa, which is freely draining meltwater to the edge of the ice body along a subglacial conduit. If magma contacts liquid water under these low-pressure conditions, we expect a vigorous phreatomagmatic eruption with pyroclast velocities of approximately 100 m s^{-1} [*Graettinger and Valentine,* 2017; *Parfitt and Wilson,* 2008].

3.2 Vertical ice ablation rate

In this section we estimate the vertical ice ablation rate resulting from impact damage by large pyroclasts (assumed to behave as solids) on the ice roof of a subglacial cavity. Consider a subglacial eruption that produces pyroclasts of various sizes that impact uniformly on the cavity roof over a zone of width w. Let the pyroclast mass flux per unit length of fissure in a given size bin be f *kg* s^{-1} m^{-1}. The number flux in that size bin is thus f/m, where m is the mass of a single pyroclast.

From equation (3), the crater volume V for a single impact is given by $V = 1.15\ m\ (\delta u^2/Y)/\rho$. We assume that the cumulative effect of multiple impacts can be approximated by the sum of the effects of single impacts. Thus, the volumetric rate of ice removal by impact damage per unit length of fissure is given by $1.15\ f\delta u^2/(\rho Y)$ and is independent of pyroclast mass (and size). For an impact zone of width w, the ablation rate of the ice cavity roof is given by $1.15\ f\delta u^2/(\rho Y w)$. We evaluate this expression with ice density ρ of 910 kg m^{-3} and compressive strength Y of 5.7 MPa (at 0 °C), together with pyroclast density δ and velocity u of 3,000 kg m^{-3} and 100 m s^{-1} respectively. The ice ablation rate in m h^{-1} is then given by $24\ f/w,$ where f is the mass flux of pyroclasts (kg s^{-1} m^{-1}) sufficiently large to cause ice fragmentation and *w* is the width of the impact zone in m.

For comparison with models of heat transfer within a liquid water-dominated cavity under glaciostatic pressure [*Woodcock et al.,* 2014], we develop an illustrative case numerically in this section, based on the inferred eruption rate and pyroclast size distribution for the Gjálp 1996 eruption [*Gudmundsson,* 2003; *Gudmundsson et al.,* 2004]. Thus, we use a total pyroclast flux of 2000 kg s^{-1} per m length of fissure and assume, to be conservative, that 7.5% of these pyroclasts, half of the 15 wt % greater than 8 mm diameter found by [*Gudmundsson,* 2003], are sufficiently large to cause impact damage of the ice roof. In this case the flux *f* is 150 kg s^{-1} m^{-1}.

The width of the impact zone *w* depends on the cavity height and the "spread" of the large pyroclasts. For a cavity height of 50 m and a "spread" half-angle of 20° the width is 36 m. The corresponding vertical linear ablation rate is 100 m h^{-1}. Thus, it appears that high rates of ice ablation from the impact damage from large pyroclasts are possible, provided that the mechanism can be sustained.

Vertical linear ice ablation rates are critically dependent on the "spread" half-angle of the large pyroclasts. However, the total ice fragmentation rate (and thus the overall rate of cavity growth) is independent of "spread". Furthermore, impacts distributed over the whole roof and walls of the cavity serve to roughen the surface, enhancing both heat transfer area and convective steam heat fluxes, although the contribution to ice ablation by steam condensation is an order of magnitude less than the contribution by pyroclast impact [*Woodcock et al*., 2015].

4 The fate of ice fragments removed by pyroclast impact

Ice excavated by the impact of large pyroclasts will begin to melt as it falls from the ice cavity roof and then continue to melt by contact with hot material around the vent. The pyroclast impact mechanism will be sustained provided that meltwater is generated at a great enough rate to produce a mixture of pyroclasts, ice and liquid water with sufficient mobility to flow out of the cavity.

We assume that the mixture has sufficient mobility if it contains at least 50% volume of liquid water. The value of 50% corresponds to the boundary between a debris flow and a hyperconcentrated flow (which, according to *Vallance* [2000], has "fluvial" behaviour but a high sediment loading). This value is for open-channel flow of a solid-liquid mixture in which all of the solids, apart from pumice, have a higher density than the liquid; in contrast, flow out of the cavity will be through a subglacial conduit, with some of the solid phase (ice) having a lower density than water below 150°C [*Rogers and Mayhew*, 1980].

We estimate the fraction of ice fragments that must melt to produce 50% volume liquid as follows. The ratio of ice fragment mass to large pyroclast mass is 6.1 (equation 3) for a pyroclast impact velocity of 100 m s^{-1}. Thus, the mixture comprises 2000 kg s^{-1} m^{-1} of pyroclasts (including 150 kg s^{-1} m^{-1} sufficiently large to fragment ice) together with 915 kg s^{-1} m^{-1} of ice fragments, part of which needs to melt. In addition, approximately 90 kg s^{-1} m^{-1} of meltwater is produced, independently of ice impact, by steam condensation on the walls and roof of the cavity. The total liquid water flow, for 50% volume in the mixture, needs to be 844 kg s^{-1} m^{-1}. The fraction of ice fragments that must melt is thus 0.82.

The fraction of ice fragments that melt before landing may be determined by comparing the time required to melt a fragment of a given size to the time available for melting. For simplicity, we assume that ice fragments are spherical and melt initially by convective steam condensation with a heat transfer coefficient of 1 kW m^{-2} K^{-1} as they fall. The corresponding linear melt-rate is thus approximately 0.3 mm s^{-1}. To estimate the time available, we assume that ice fragments fall with their initial terminal velocity through stagnant fluid from the roof of a 50 m high ice cavity. For a 3 mm ice sphere, the time available during fall is 5 s, compared to the time required for melting of 3.5 s.

Ice fragments of 3 mm or less should melt during their fall from the ice cavity roof; these comprise 80 % of the total mass in the experiments described in *Kato et al.* [1995] (Section 2.1.2). Thus, in this example case, there is almost sufficient melting of ice fragments during fall to produce a mixture of sufficient mobility; there should be no accumulation of ice in the cavity and pyroclast impact may continue as long as the eruption is sufficiently energetic to reach the cavity roof.

There are two conditions under which the ice cavity may accumulate ice. One condition arises when the resulting ratio of ice fragment mass to pyroclast mass is so great that the initial heat content of the magma is incapable of producing sufficient meltwater for transport of pyroclasts and ice out of the cavity. The second condition is envisaged to occur if internal explosions or pyroclast impact produces a network of fractures in the ice roof. These fractures may promote the stoping of large ice fragments from the ice roof. Although these ice blocks are likely to break up on landing, the extent to which they melt is difficult to quantify.

5. Discussion

5.1 The nature of the pyroclasts

In vapour dominated ice cavities, condensation of steam produces a liquid film of condensate and meltwater on the walls and roof of the cavity. Large pyroclasts are those that are able to disrupt this water film on the ice surface and are too heavy to be retained by surface tension. Additionally, mechanical and thermal coupling to the cavity fluid (predominantly water vapour) is weak. Such pyroclasts are likely to be larger than 10 mm in diameter and have undergone a degree of cooling dependent on their size and extent of interaction with water. The consequence is that large pyroclasts impact ice with variable rheology. Solid pyroclasts will interact elastically with the ice. Hotter pyroclasts may dissipate impact energy by deforming inelastically, a process that also increases impact duration and reduces the stress applied to the ice; in this case fuel-coolant interactions may become possible [*Wilson et al.*, 2013].

The behaviour of pyroclasts with cooler carapaces and hotter cores is complex to quantify. Pyroclasts impacting a surface will be subject to high strain rates, for example a pyroclast travelling at 100 m s^{-1} coming to a halt in 0.01 m undergoes a strain rate of order 10^4 s^{-1}. To behave as a solid the outer carapace would need an effective viscosity exceeding order 10^4 Pa s [*Papale*, 1999]. Basalt typically has a dry eruption viscosity in the region 10^2 - 10^4 Pa s. Radiation and any interaction with water is likely to significantly increase the viscosity of the pyroclast surface region during rapid cooling, thereby increasing the likelihood that pyroclasts behave as dynamic solids during impact.

5.2 Pyroclast velocity on impact versus velocity at vent

As pyroclasts travel from the eruption vent to impact on the ice cavity roof there is the potential for significant deceleration by gravity and fluid drag. For a 50 m high cavity and a pyroclast velocity at the vent of 100 m s^{-1}, gravity alone reduces the impact velocity to 95 m s^{-1}. For a stagnant cavity vapour, the combined effect of fluid drag and gravity on velocity is severe and dependent on pyroclast diameter. Thus, if the cavity vapour pressure is 0.2 MPa the velocity of a 32 mm diameter pyroclast is approximately 50 m s^{-1} at the cavity roof, while an 8 mm diameter pyroclast fails to reach the cavity roof. In reality, the cavity vapour will not be stagnant, but will comprise a jet of gas and pyroclasts above the vent that is decelerated principally by entrainment of cavity vapour. We make a more realistic estimate of pyroclast velocity at the cavity roof by adapting the integral plume model developed by *Woods* [2013].

The integral plume model solves the mass, momentum, and energy conservation equations for a jet of gas and pyroclasts that progressively entrains the vapour surrounding the jet. We have modified these equations for momentum-dominated jets by neglecting the buoyancy terms. Furthermore, because the plume transit time in the cavity is short compared with the pyroclast cooling time, we have assumed thermal disequilibrium between pyroclasts and vapour. These assumptions simplify the differential equations considerably and allow a straightforward numerical solution. Table 3 summarises the results of calculations, in which basaltic magma at 1100 °C and liquid water interact phreatomagmatically to produce an initial jet of pyroclasts and steam. The integral plume model assumes that pyroclasts and gas within the jet move at the same velocity; in reality, pyroclasts will have their velocities reduced by their terminal velocities. For a cavity containing steam at 0.2 MPa, this reduction is approximately 20 m s^{-1} for a 16 mm pyroclast and is proportional to the square root of the pyroclast diameter for turbulent drag [*Kay and Nedderman*, 1985].

Table 3. Eruption jet velocity (m s^{-1}) at 50 m above the vent.

Initial velocity (m s^{-1})	Initial temperature of jet/° C		
	900	700	500
100	78	68	64
150	117	102	96
200	156	136	128

We conclude that there is some reduction in pyroclast velocity between vent and roof. Equation (3) indicates that the mass of the ice produced by cratering is proportional to the square of the velocity; thus a 30% reduction in velocity will halve the ice ablation rates.

5.3 Downward movement of ice cavity roof by ductile flow

In the absence of any progressive downward movement of the ice cavity roof, or of any build-up of a subglacial volcanic edifice within the cavity, the distance between the volcanic vent and the ice cavity roof would increase as ablation of the roof proceeds. The resulting decrease in pyroclast impact velocity (Section 5.2) would cause a decrease in ice fragmentation rate. Thus, one might expect the cavity height to approach a limit, assuming constant eruption rate, pyroclast size distribution and velocity at the vent. In reality, the ice cavity roof is likely to move downwards by ductile ice flow.

We estimate likely rates of downward movement of an ice cavity roof as follows. *Gudmundsson et al*. [2004] examined ice cauldron development for the Gjálp eruption by modelling the ice above the cavity roof as a plug that moves downwards in response to ductile ice deformation on the vertical margins of the plug. In this model the weight of the ice plug is balanced by the force of the cavity water pressure acting on the base of the plug and the ductile shear stresses acting on the non-crevassed sides of the plug. *Gudmundsson et al*. [2004] used the resulting equation, together with observations of the rate of ice cauldron development, to estimate the cavity water pressure.

If the cavity fluid pressure is known, the same equation can be used to estimate the downward velocity of the ice plug and thus the ice roof, irrespective of the phase of the cavity fluid. For a vapour-filled cavity with a fluid pressure of 0.2 MPa, the force acting on the base of the plug is small compared with its weight; in this case the downward velocity is almost independent of the ice depth. Apart from changing the cavity fluid pressure, we use the same data as *Gudmundsson et al.* [2004] to evaluate the equation. The resulting downward velocity of the cavity roof is approximately 60 m h^{-1}; the same order of magnitude as the vertical ice ablation rate estimated in Section 3.2.

6. Conclusions

(1) We propose and evaluate a mechanism with potential for rapid ablation of the ice overlying a subglacial, mafic volcanic vent that involves the impact of large pyroclasts

on the ice surfaces of depressurised, water vapour dominated cavities that surround the vent. Such impacts are likely to cause considerable fracturing and fragmentation of the overlying ice and thus increase the heat transfer area available for ice-melt. This mechanism has not, to our knowledge, been explored previously in the literature.

(2) Ice ablation rates of order 100 m h^{-1} are predicted, for typical pyroclast velocities, provided that the mechanism is sustained.

(3) The thermal energy of the eruption, together with the size of the ice fragments produced, is sufficient to prevent accumulation of fractured ice within the cavity.

(4) Upward ablation of the ice cavity roof results in a progressive decrease in pyroclast impact velocity that is partly compensated by downward movement of the roof by ductile ice flow.

(5) This ice ablation mechanism may be relevant to subglacial eruptions beneath ice on the relatively steep slopes of ice-covered stratovolcanoes, where steepness of slope and ice thickness are favourable for rapid drainage of meltwater by gravity and consequent depressurisation of the cavity.

Acknowledgement

We thank Karoly Nemeth and an anonymous reviewer for detailed comments during review that have enabled us to improve the paper. We also thank the editor Sonia Calvari for her comments. We are grateful to Magnus Tumi Gudmundsson for reading and commenting on earlier versions of this paper.

References

Björnsson, H. (1975), Subglacial water reservoirs, jökulhlaups and volcanic eruptions, *Jökull, 25*, 1-14.

Björnsson, H., Pálsson, F., and Gudmundsson, M.T. (2000), Surface and bedrock topography of the Mýrdalsjökull ice cap, Iceland: The Katla caldera, eruption sites and routes of jökulhlaups, *Jökull, 49*, 29-46.

Burchell, M.J., and Johnson, E. (2005), Impact craters on small icy bodies such as icy satellites and comet nuclei. *Monthly Notices of the Royal Astronomical Society 360*, 769-781.

Croft, S.K., Kieffer, S.W., and Ahrens, T.J. (1979), Low-velocity impact craters in ice and ice-saturated sand with implications for Martian crater count ages, *Journal of Geophysical Research 84*, 8023-8032.

Dellino, P., Gudmundsson, M.T., Larsen, G., Mele, D., Stevenson, J.A., Thordarson, T., and Zimanowski, B. (2012), Ash from the Eyjafjallajökull eruption (Iceland): Fragmentation processes and aerodynamic behaviour, *Journal of Geophysical Research, 117*, B00C04.

Gudmundsson, M.T. (2003), Melting of ice by magma-ice-water interactions during subglacial eruptions as an indicator of heat transfer in subaqueous eruptions, in *Explosive Subaqueous Volcanism, Geophysical Monograph Series,* vol. 140, edited by J.D.L. White, J.L. Smellie, and D.A. Clague, pp. 61-72, AGU, Washington, D.C.

Gudmundsson, M.T., Sigmundsson, F., Bjornsson, H., and Hognadottir, T. (2004), The 1996 eruption at Gjálp, Vatnajökull ice cap, Iceland: efficiency of heat transfer, ice deformation and subglacial water pressure, *Bulletin of Volcanology*, *66*, 46-65.

Gudmundsson, M.T., Larsen, G., Hoskuldsson, A., and Gylfason, A.G. (2008), Volcanic hazards in Iceland, *Jökull, 58*, 251-268.

Gudmundsson, M.T., Janebo, M.H., Larsen, G., Hognadottir, T., Thordarsson, T., Gudnason, J., and Jonsdottir, T. (2021), The explosive, basaltic Katla eruption in 1918, south Iceland: II. Isopach map, ice cap deposition of tephra and layer volume, *Jökull* 71, 21-38.

Harris, A.J.L., Gurioli, L., Hughes, E.E., and Lagreulet, S. (2012), Impact of the Eyjafjallajökull ash cloud: A newspaper perspective, *Journal of Geophysical Research, 117*, B00C08.

Holsapple, K.A. (1993), The scaling of impact processes in planetary sciences. *Annual Review of Earth and Planetary Sciences 21*,333-373.

Holsapple, K.A., and Schmidt, R.M. (1982), On the scaling of crater dimensions 2. impact processes. *Journal of Geophysical Research 87*, 1849-1870.

Iijima, Y., Kato, M., Arkawa, M., Maeno, N., Fujimura, A., and Mizutani, H. (1995), Cratering experiments on ice: dependence of crater formation on projectile material and scaling parameter. *Geophysical Research Letters 22*, 2005-2008.

Kato, M., Iijima, Y., Arakawa, M., Okimura, Y., Fujimura, A., Maeno, N., and Mizutani, H. (1995), Ice-on-ice impact experiments. *Icarus 113*, 423-441.

Kay, J. M., and Nedderman, R. M. (1985), *Fluid mechanics and transfer processes*, Cambridge University Press, Cambridge, 602pp., first edition.

Lange, M.A., and Ahrens, T.J. (1987), Impact experiments in low-temperature ice. *Icarus 69*, 506-518.

Larsen, G., Janebo, M.H., and Gudmundsson, M.T. (2021), The explosive, basaltic Katla eruption in 1918, south Iceland: I. Course of events, tephra fall and flood routes, *Jökull,71,* 1-20.

Limonta, S., Trisolini, M., Frey, S., and Colombo, C (2021), Fragmentation model and strewn field estimation for meteoroids entry, *Icarus, 367*, 114553.

Magnússon, E., Gudmundsson, M.T., Roberts, M.J., Sigurdsson, G., Höskuldsson F., and Oddsson, B. (2012), Ice-volcano interactions during the 2010 Eyjafjallajökull eruption, as revealed by airborne imaging radar. *Journal of Geophysical Research 117*, B07405.

Middleton, G.V., and Wilcock, P.R. (1994), *Mechanics in the earth and environmental sciences*. Cambridge University Press, Cambridge, 459pp, first edition.

Nye, J.F. (1976), Water flow in glaciers: jökulhlaups, tunnels and veins, *Journal of Glaciology, 17*, 181-210.

Papale, P. (1999), Strain-induced magma fragmentation in explosive eruptions, *Nature, 397*, 425-428.

Parfitt, E.A., and Wilson, L. (2008), *Fundamentals of Physical Volcanology*, Blackwell, Oxford, 459pp, first edition.

Paterson, W.S.B. (2002), *The physics of glaciers*, Butterworth-Heinemann, Oxford, 496pp, third edition.

Petrovic, J.J. (2003), Mechanical properties of ice and snow. *Journal of Materials Science 38*, 1-6.

Rogers, G.F.C., and Mayhew, Y.R. (1980), *Thermodynamic and Transport Properties of Fluids (SI Units),* Blackwell Publishing, Oxford, 24pp, third edition.

Shrine, N.R.G., Burchell, M.J., and Grey, I.D.S. (2002), Velocity scaling of impact craters in water ice over the range 1 to 7.3 km s^{-1}. *Icarus 155*, 475-485.

Smellie, J. L. (2002), The 1969 subglacial eruption on Deception Island (Antarctica): events and processes during an eruption beneath a thin glacier and implications for volcanic hazards, in *Volcano-Ice Interaction on Earth and Mars,* edited by J.L. Smellie and M.G. Chapman, *Geological Society Special Publications, 202*, 59-79.

Susorney, H. C. M., Barnouin, O. S., Stickle, A. M., Ernst, C. M., Crawford, D. A., and Cintala, M. J. (2017), The role of target heterogeneity in impact crater formation: numerical results, *Procedia Engineering 204*, 421–428.

Vallance, J.W. (2000), Lahars, in: *Encyclopaedia of Volcanoes (first edition)*, edited by H. Sigurdsson, pp. 601–616, Academic Press, San Diego.

Wilson, L., and Head, J.W. (2002), Heat transfer and melting in subglacial basaltic volcanic eruptions: implications for volcanic deposit morphology and meltwater volumes, in *Volcano-Ice Interaction on Earth and Mars,* edited by J.L. Smellie and M.G. Chapman, *Geological Society Special Publications, 202*, 5-26.

Wilson, L., Smellie, J.L., and Head, J.W. (2013), Volcano-ice interactions, in *Modelling Volcanic Processes: The Physics and Mathematics of Volcanism*, edited by S.A. Fagents, T.K.P. Gregg and R.M.C. Lopes, pp. 275-299, Cambridge University Press.

Woodcock, D.C, (2016), Magma -ice heat transfer in subglacial volcanism, Ph.D. Thesis, Lancaster Environment Centre, Lancaster University, UK, 322pp.

Woodcock, D.C., Gilbert, J.S., and Lane, S.J. (2012), Particle-water heat transfer during explosive volcanic eruptions, *Journal of Geophysical Research: Solid Earth, 117*, B10205.

Woodcock, D.C., Lane, S.J., and Gilbert, J.S. (2014), Ice-melt rates in liquid-filled cavities during explosive subglacial eruptions, *Journal of Geophysical Research: Solid Earth, 119*, B10617.

Woodcock, D.C., Gilbert, J.S., and Lane, S.J. (2015), Ice-melt rates by steam condensation during explosive subglacial eruptions, *Journal of Geophysical Research: Solid Earth*, *120*, B11619.

Woods, A.W. (2013), Sustained explosive activity: volcanic eruption columns and Hawaiian fountains, in *Modelling Volcanic Processes*, edited by S.A. Fagents, T.K.P. Gregg, and R.M.C. Lopes, pp 153-172, Cambridge University Press.